VNU Journal of Science: Mathematics - Physics

Journal homepage: https://js.vnu.edu.vn/MaP

Original Article

Photoluminescence Emission and Raman Vibration Properties of Asymmetric Mn^{2+}-Doped ZnO Nanoparticle Fabricated by a Solvothermal Method

Nguyen Xuan Sang[1,*], Nguyen Thi Phuong Anh[2], Nguyen Duy Dung[2], Nguyen Hoang Cao Huy[2], Nguyen Huu Tho[2], Luu Thi Lan Anh[3]

[1]*Department of Electronics and Telecommunication, Saigon University, 273 An Duong Vuong, District 5, Ho Chi Minh City, Vietnam*

[2]*Department of Natural Sciences Education, Saigon University, 273 An Duong Vuong, District 5, Ho Chi Minh City, Vietnam*

[3]*School of Engineering Physics, Hanoi University of Science and Technology, 1 Dai Co Viet, Hanoi, Vietnam*

Received 28 June 2019, Accepted 06 August 2019

Abstract: In this study, Mn^{2+}-Doped ZnO nanoparticle with hexagonal wurtzite phase was fabricated by a solvothermal method where various contents of Mn ion were *in situ*-doped in ZnO nanostructure. The crystal structure and morphological properties of the nanoparticle were investigated by X-ray diffractometry, Raman spectroscopy and transmission electron microscopy. The photoluminescence (PL) measured at room temperature showed red-shift of near-band-to-band emission and the evolution of visible emissions in the doped samples. The study also analyzed the PL characteristics of synthesized samples and revealed the role of dopant Mn^{2+} to defect states of ZnO.

Keywords: Mn ion, ZnO, solvothermal synthesis, nanoparticle, photoluminescence.

1. Introduction

Zinc oxide (ZnO), a wide and direct bandgap (~3.37 eV) with large exciton binding energy (60 meV) at room temperature, has been attracted a huge interest from scientists worldwide as a promising

*Corresponding author.
Email address: sangxuannguyen@gmail.com

https//doi.org/ 10.25073/2588-1124/vnumap.4344

material for optoelectronic and photocatalytic applications [1, 2]. Recently, due to its availability, eco-friendly environment, safety, stability, ZnO material has been got attention as an excellent photocatalyst [3, 4]. There are several problems needed to solve in advance for practical application of the material. Firstly, ZnO has a large exciton binding energy, so excited carrier lifetime is not long enough to degrade organic compounds. Secondly, the large bandgap means the working irradiation light for photocatalytic activity must be in the range of ultra-violet. However, in the natural sunlight, there is a small amount of UV-light ~3%. Hence the bandgap engineering of ZnO has been intensively investigated such as doping ZnO with other elements [5-9], coating ZnO with other materials [10, 11]. Recently, S. Choi *et al.*[7] found that when ZnO doped with transition metal ion Cu^{2+}, the photocatalytic activity of ZnO was improved thanks to the separation of the excited carrier. Recently, we have shown that the Cr^{3+} could be play as an electron trap center in the hydrothermal ZnO doped Cr samples [5]. It means that the photoelectrons were trapped then would leave holes without recombination.

In this work, we fabricated ZnO doped Mn^{2+} by a facile solvothermal method. Crystal structure and morphological properties were characterized by D8 Advance X-ray diffractometry (XRD, Bruker), transmission electron microscopy (TEM, Jeol 1600) and Raman spectroscopy (533 nm, Renishaw). The optical properties were investigated by room temperature photoluminescence system (Horiba Nanolog) with an excited source of 325 nm wavelength from Xe lamp. The revolution of PL emission was analyzed by deconvolution the emission spectra, and then the role of ion Mn^{2+} was inferred.

2. Experimental

ZnO materials were synthesized by a solvothermal method. Zinc acetate dihydrate $Zn(CH_3COO)_2.2H_2O$ (≥ 99%) and triethanoldiamin (TEA) – $C_6H_{15}NO_3$ (≥ 99%) was supplied by Xilong, China; whereas Ethanol – C_2H_5OH (≥ 99%) and $Mn(CH_3COO)_2.4H_2O$ (≥ 99%) were purchased from Merck and Kanto, respectively. All the chemicals were purchased and used as received without further purification. The synthesis procedures are as follows: 0.07 mol $Zn(CH_3COO)_2.2H_2O$ was dissolved in 70 mL of ethanol under magnetic stirring at room temperature (RT). Then, an amount of TEA was added and stirred in 1 h at 60 ℃. In the synthesis process, $Mn(CH_3COO)_2.4H_2O$ was added dropwise to obtain proper molar concentration of Mn^{2+} ions in ZnO: 1.0 and 3.0 at.%, were named as ZnO:Mn1 and ZnO:Mn3, respectively. After that, the solution was poured in a teflon-lined autoclave and treated at 150 ℃ in 18 h. The autoclave is cooled naturally to room temperature (RT) and the white precipitate was washed with distilled water until pH reaches 7. Finally, the powder was dried at 100 ℃ for 5h.

3. Results and discussion

3.1. XRD patterns

In order to investigate the crystalline structure of ZnO materials, X-ray diffraction (XRD) pattern was carried out at RT. The results are shown in Figure 1. The lattice parameters (*a*, *c*) were obtained by Bragg's law:

$$n\lambda = 2d\sin\theta \quad (1)$$

(n=1, λ is the wavelength of incident X-ray used, 0.15418 nm) and the following evaluation, which is defined for hexagonal phase:

$$\frac{1}{d^2} = \frac{4}{3}\left[\frac{h^2+hk+k^2}{a^2}\right] + \frac{l^2}{c^2} \quad (2)$$

Where *d* is the distance between two consecutive parallel planes and (*hkl*) are the Miller indexes.

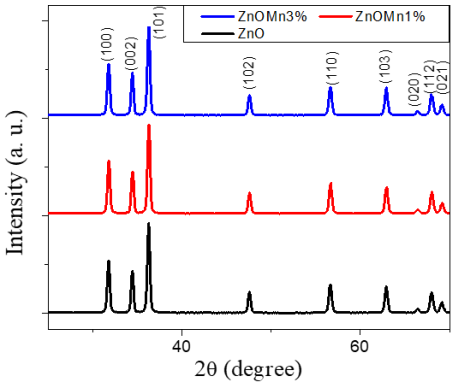

Figure 1. XRD patterns of as-prepared ZnO and Mn doped ZnO.

In the pure ZnO pattern, all the expectable Bragg angles for wurtzite phase at faces of(100), (002), (101), (102), (110), (103), (200), (112) and (201) were observed at approximately 2θ = 31.77°; 34.43°; 36.27°; 47.58°; 56.65°; 62.91°; 67.97°; 68.08° and 69.13°. The calculated lattice parameters of pure ZnO are *a* = 0.3252 and *c* = 0.5206 which are in fine agreement with *JCPDS No.36-1451 card.* There was no extra peak from secondary phases in doped samples, ZnO:Mn1 and ZnO:Mn3, indicated that materials obtained in this study were highly single phase hexagonal wurtzite. The XRD patterns of doped samples were identical to the pure ZnO indicating the average crystal size of ZnO:Mn1 and ZnO:Mn3 are the same in comparison to as-prepared ZnO. We assumed that the nanoparticle of ZnO itself has an excellent doping efficiency although the dopant ion (0.083 nm in radius) is larger than the host ion Zn^{2+} (0.074 nm) [12].

3.2. Transmission Electron Microscope (TEM) analysis

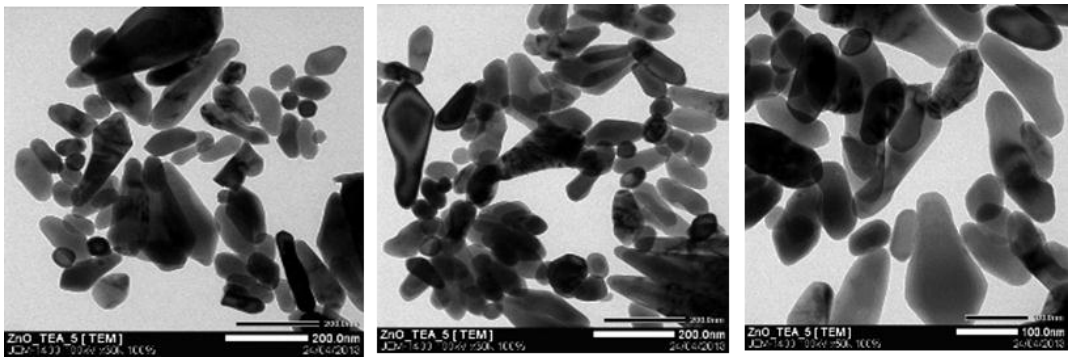

Figure 2. TEM images of as-preparedZnO.

The morphology of ZnO nanostructured was characterized by TEM micrographs, as shown in fig. 2. TEM images showed that ZnO nanoparticles were mainly asymmetric and formed in different shapes. In general, the particles were both in spherical and capsule-like shapes with the size of ~50 nm in width and ~100 nm.

3.3. Raman spectra

To investigate the information of structure disorder and dopant in crystalline materials, Raman spectra was carried out at RT. Furthermore, Raman is a nondestructive and superior method for detecting the diffusion of dopant ions into the host lattice. Figure 3 shows Raman spectra of as-prepared ZnO, ZnO:Mn1 and ZnO:Mn3 samples. ZnO wurtzite was classified in space group $P6_3mc$. The zone center optical phonons are following the equation: $\Gamma_{opt} = A_1 + E_1 + 2E_2 + 2B_1$, where B_1 modes are silent; A_1 and E_1 are polar modes and splitted into TO and LO phonons, both Raman and infrared active; whereas E_2 modes (E_2^{high} and E_2^{low}) are non-polar and Raman active only[13]. The presence of impurities and/or defects could have an effect on both A_1 (LO) andE_1 (LO). Particularly, E_1 (LO) is affected strongly[14]. The assignation and wavenumbers (based on study by R.Cuscó *et al.*[14]) of the first and second-order are listed in Table 1.

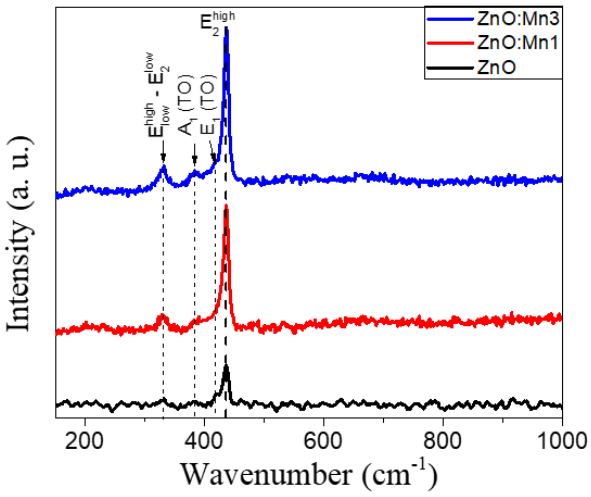

Figure 3. Raman spectra of as-prepared ZnO and Mn-doped ZnO samples.

In general, Raman vibration modes were sharper and more intensive when Mn content increased. According to Fig. 3, the most intensive peak in the Raman spectra was E_2^{high} at ~ 436 cm^{-1} which assigned to the oxygen vibration[14]. When Mn^{2+} ions introduced, the E_2^{high} increased but remained the same position along with the absence ofE_1 (LO) modes which related to oxygen vacancies[15], suggested that defects due to oxygen, such as excess oxygen and/or interstitial oxygen (O_i) were increased. In addition, there was a weak peak at approximately 660 cm^{-1} which related to the vibration of bonding between Mn and O in the crystal lattice was observed in Raman spectra of ZnO:Mn1 and ZnO:Mn3. It is worth to note that the XRD results indicated no secondary phase observed, we assumed that the Mn^{2+} ions could successfully substitute Zn^{2+} in the crystal.

Table 1. The wavenumbers (in cm^{-1}) of the 1st and 2nd order Raman spectra found in pure ZnO and Mn-doped samples.

	Wavenumber (cm^{-1})			
Mode	Ref.[14]	Pure ZnO	ZnO:Mn1	ZnO:Mn3
E_2^{high} - E_2^{low}	333	333	329	332
A_1(TO)	378	385	378	383
E_1 (TO)	410	418		
E_2^{high}	438	436	436	436
A_1 (LO)	574			
E_1 (LO)	590			

3.4. Photoluminescence (PL) study

To study the optical properties and defects that exist in the band gap of the materials, we measured photoluminescence spectra at room temperature. In principle, the UV peak in the PL spectra is associated to the near band-to-band emission (NBE), while the visible emission originates from the defect levels, which includes zinc vacancies (V_{Zn}), interstitial zinc (Zn_i), interstitial oxygen (O_i) and lattice defects relating to oxygen and zinc.

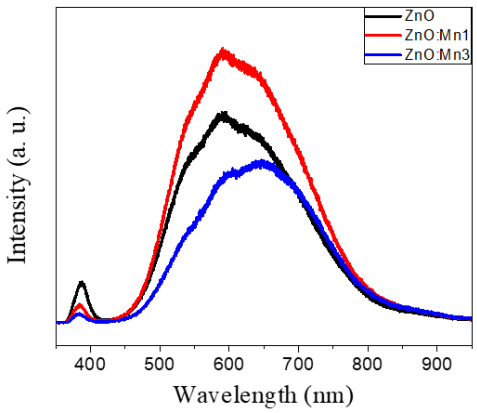

Figure 4. Room temperature photoluminescence spectra of synthesized samples.

Figure 4 illustrates the PL spectra of as-prepared and doped ZnO samples. As shown in Fig. 4, the PL spectra of as-prepared ZnO, ZnO:Mn1 and ZnO:Mn3 showed not only an NBE emission centered at 387 nm (3.20 eV), 385 nm (3.22 eV) and 384 nm (3.23 eV), respectively; but also a broad intense deep-level (DL) at 589 nm (2.11 eV) in as-synthesized ZnO, 591 nm (2.10 eV) in ZnO:Mn1, 596 nm (2.08 eV) and 647 nm (1.92 eV). When Mn^{2+} ions were introduced, the NBE emissions were slightly red-shifted, which revealed that the crystallinity was improved. Besides, at 1.0 at.% Mn^{2+} concentration, the intensity of UV peak decreased and that of the DL emission increased. This could have resulted from Mn^{2+} ions acting as trapped centers in the bandgap of ZnO nanostructure. Moreover, when Mn^{2+} concentration was increased to 3.0 at.%, both NBE and DL emissions decreased. This luminescence quenching might due to the outside covering of the ZnO nanoparticles. We assumed that Mn 1.0 at.% concentration is the best doping yield.

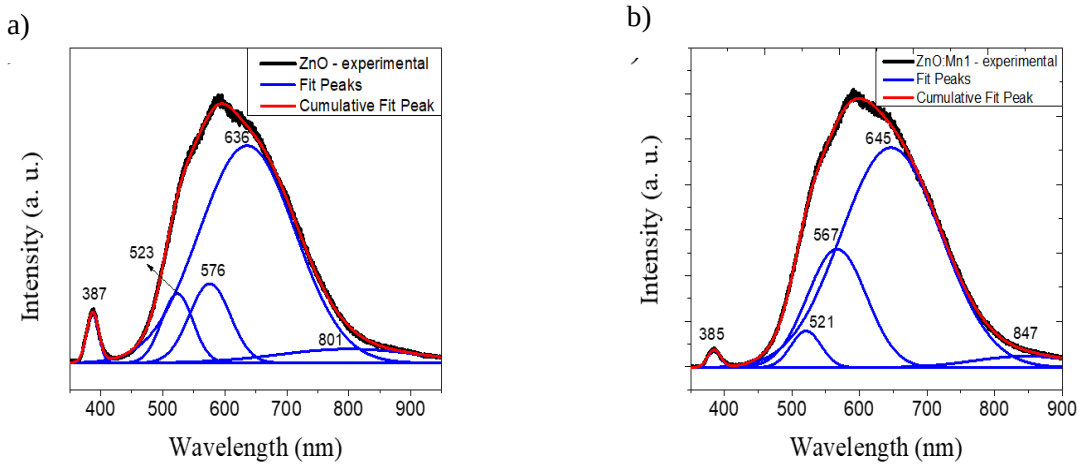

Figure 5. Photoluminescence spectra of: a) as-synthesized ZnO and b) ZnO:Mn1

In order to study bandgap structure, deep-level emissions in PL spectra of ZnO were Gaussian-resolved into four emissions, which belong to green luminescence: 523 nm (2.37 eV) in ZnO sample and 521 nm (2.38 eV) in ZnO:Mn1 sample; yellow – red regions: ZnO at 576 nm (2.15 eV), 636 nm (1.95 eV); and ZnO:Mn1 at 567 nm (2.19 eV), 645 nm (1.92 eV); and infrared radiation (IR) at 801 nm (1.55 eV) in ZnO, 847 nm (1.46 eV) in ZnO:Mn1, as shown in Fig. 5. Firstly, according to studies by Vanheusden *et al.*[16,17], correlation between the intensity of the green luminescence and the concentration of V_O based on the observation of a line with $g \sim 1.96$ in EPR measurement proposed for green emission. In addition, Leiter *et al.*[18, 19] reported the green band around 2.45 eV with oxygen vacancies based on optically detected magnetic resonance experiments. Still in debate, Reynolds *et al.*[20] and Kohan *et al.*[21] have suggested that transitions between the conduction band (or shallow donor) and the V_{Zn} are the source of green band. Based on Janotti *et al.* [22] calculation, this transition would give rise to luminescence around 2.4 – 2.5 eV. Moreover, a strong argument in favor of zinc vacancies had been provided by strong passivation of the green emission by hydrogen plasma treatment in experiments of Sekiguchi *et al.* [23] and Lavrov *et al.* [24] whose works simultaneously observed an increase in vibrational modes associated with hydrogenated zinc vacancies. In this study, it could possibly conclude that the green luminescence was originated from V_{Zn}. When the dopant ions diffused into wurtzite lattice, V_{Zn} in unit cells was substituted by Mn^{2+}, which resulted in the intensity of emission centered in green region decreased. Secondly, peaks at yellow region, which centered at 576 nm (2.15 eV) in pure ZnO and 567 nm (2.19 eV) in ZnO:Mn1, might be contributed to O_i or other defect complexes [25, 26]. Thirdly, the dominant emission peaks appeared in ZnO and 1.0 at.% Mn doped ZnO samples were in red region at 636 nm (1.95 eV) and 645 nm (1.92 eV), respectively, would possibly contribute to $O_{i\,(oct)}^{2-}$ defect [22]. Finally, in this study, we also obtained an infrared emissions centered at 801 nm (1.55 eV), 847 nm (1.46 eV) in ZnO, ZnO:Mn1 PL spectra, respectively. These emissions are from radiative transitions of intrinsic defects.

4. Conclusions

In conclusion, the asymmetrical ZnO nanoparticles doped and undoped with Mn^{2+} were successfully prepared by a simple sovolthermal method. The doping efficiency with ion Mn^{2+} was

high then the crystalline structure of the doped samples was not significantly changed. The photoluminescence of synthesized samples was investigated and showed the effect of Mn content in the ZnO matrix. In general, the UV emission intensity of ZnO was decreased when the content of the dopant Mn^{2+} increased. The red-shift of the UV emission when introducing Mn^{2+} in the ZnO matrix indicated that the electrons in the conduction band or near deep donor level of ZnO were captured by the dopant ions. Hence the conduction band would be up-shifted.

Acknowledgements

This research is funded by Saigon Universityfor basic research under grant number CS2019-46

References

[1] J. Miao, B. Liu, II–VI semiconductor nanowires, Semiconductor Nanowires,Woodhead Publishing, London (2015) 3-28. https://doi.org/10.1016/b978-1-78242-253-2.00001-3

[2] M. Samadi, M. Zirak, A. Naseri, E. Khorashadizade, A.Z. Moshfegh, Recent progress on doped ZnO nanostructures for visible-light photocatalysis, Thin Solid Films 605 (2016) 2-19. https://doi.org/10.1016/j.tsf.2015.12.064

[3] M.R.D. Khaki, M.S. Shafeeyan, A.A.A. Raman, W. Daud, Application of doped photocatalysts for organic pollutant degradation - A review, Journal of Environmental Management 198 (2017) 78-94. https://doi.org/10.1016/j.jenvman.2017.04.099

[4] K.M. Lee, C.W. Lai, K.S. Ngai, J.C. Juan, Recent developments of zinc oxide based photocatalyst in water treatment technology: A review, Water Research 88 (2016) 428-448. https://doi.org/10.1016/j.watres.2015.09.045

[5] N.X. Sang, N.M. Quan, N. H. Tho, N.T. Tuan, T.T. Tung, Mechanism of enhanced photocatalytic activity of Cr-doped ZnO nanoparticles revealed by photoluminescence emission and electron spin resonance, Semiconductor Science and Technology 34 (2019) 025013. https://doi.org/10.1088/1361-6641/aaf820

[6] F. Achouri, S. Corbel, L. Balan, K. Mozet, E. Girot, G. Medjahdi, M.B. Said, A. Ghrabi, R. Schneider, Porous Mn-doped ZnO nanoparticles for enhanced solar and visible light photocatalysis, Materials & Design 101 (2016) 309-316. https://doi.org/https://doi.org/10.1016/j.matdes.2016.04.015

[7] S. Choi, J.Y. Do, J.H. Lee, C.S. Ra, S.K. Kim, M. Kang, Optical properties of Cu-incorporated ZnO (Cu x Zn y O) nanoparticles and their photocatalytic hydrogen production performances, Materials Chemistry and Physics 205 (2018) 206-209. https://doi.org/10.1016/j.matchemphys.2017.11.022

[8] Y. Liu, J. Yang, Q. Guan, L. Yang, Y. Zhang, Y. Wang, B. Feng, J. Cao, X. Liu, Y. Yang, M. Wei, Effects of Cr-doping on the optical and magnetic properties in ZnO nanoparticles prepared by sol–gel method, Journal of Alloys and Compounds 486 (2009) 835-838. https://doi.org/10.1016/j.jallcom.2009.07.076

[9] H. Luo, P. Dorenbos, The dual role of Cr3+ in trapping holes and electrons in lanthanide co-doped GdAlO3 and LaAlO3, Journal of Materials Chemistry C. 6 (2018) 4977-4984. https://doi.org/10.1039/C8TC01100A

[10] D. Schelonka, M. Slušná, J. Tolasz, D. Popelková, P. Ecorchard, ZnO-GO Composite with for Photocatalytic Applications, Materials Today: Proceedings 3 (2016) 2679-2687. https://doi.org/https://doi.org/10.1016/j.matpr.2016.06.012

[11] P.S. Chauhan, R. Kant, A. Rai, A. Gupta, S. Bhattacharya, Facile synthesis of ZnO/GO nanoflowers over Si substrate for improved photocatalytic decolorization of MB dye and industrial wastewater under solar irradiation, Materials Science in Semiconductor Processing 89 (2019) 6-17. https://doi.org/https://doi.org/10.1016/j.mssp.2018.08.022

[12] N.A. Putri, Y. Febrianti, I. Sugihartono, V. Fauzia, D. Handoko, Effects of Mn dope on morphological, structural and optical properties of ZnO nanorods grown by a hydrothermal method, AIP Conference Proceedings 1862 (2017) 030046. https://doi.org/10.1063/1.4991150

[13] S. Maja J Scepanovic, Raman Study of Structural Disorder in ZnO Nanopowders, Journal of Raman Spectroscopy 41 (2010) 914-921. https://doi.org/https://doi.org/10.1002/jrs.2546

[14] L.R. Cuscó, J. Ibáñez, L. Artús, Temperature dependence of Raman scattering in ZnO, Physical Review B. 75 (2007). https://doi.org/https://dx.doi.org/10.1103/PhysRevB.75.165202

[15] X.L.Xu, J.S.Chen, G.Y.Chen, B.K.Tay, Polycrystalline ZnO thin films on Si (1 0 0) deposited by filtered cathodic vacuum arc, Crystal Growth 223 (2001) 201-205. https://doi.org/https://doi.org/10.1016/S0022-0248(01)00611-X

[16] K. Vanheusden, W.L. Warren, D.R. Tallant, and J. A. Voigt, Correlation between photoluminescence and oxygen vacancies in ZnO phosphors, Applied Physics Letters 68 (1996).
https://doi.org/doi.org/10.1063/1.116699

[17] K.Vanheusden, W.L.Warren, D.R.Tallant, J.Caruso, M.J.Hampden-Smith and T.T.Kodas, Green photoluminescence efficiency and free-carrier density in ZnO phosphor powders prepared by spray pyrolysis, Journal of luminescence 75 (1997) 11-16. https://doi.org/doi.org/10.1016/S0022-2313(96)00096-8

[18] F.H. Leiter, A. Hofstaetter, D.M. Hofmann and B.K. Meyer, The Oxygen Vacancy as the Origin of a Green Emission in Undoped ZnO, Physica status solidi (b) 226 (2001) R4-R5.

[19] [19] F.Leiter, D.Pfisterer, N.G.Romanov, D.M.Hofmann and B.K.Meyera, Oxygen vacancies in ZnO, Physica B: Condensed Matter 340-342 (2003) 201-204. https://doi.org/doi.org/10.1016/j.physb.2003.09.031

[20] D.C. Reynolds, B. Jogai, J.E. Van Nostrand, R. Jonesb and J. Jennyb,Source of the yellow luminescence band in GaN grown by gas-source molecular beam epitaxy and the green luminescence band in single crystal ZnO, Solid State Communications 106 (1998) 701-704.

[21] A. F. Kohan, D. Morgan, and Chris G. Van de Walle, First-principles study of native point defects in ZnO, Physical Review B. 61 (2000). https://doi.org/doi.org/10.1103/PhysRevB.61.15019

[22] W. Anderson Janotti, Native point defects in ZnO, Physical Review B, 76 (2007) 165202.

[23] T. Sekiguchi, N. Ohashi,Y. Terada, Effect of Hydrogenation on ZnO Luminescence, Japanese Journal of Applied Physics 36 (1997) 289-291. https://doi.org/10.1143/JJAP.36.L289

[24] J.W. E. V. Lavrov, F. Börrnert, Chris G. Van de Walle, and R. Helbig, Hydrogen-related defects in ZnO studied by infrared absorption spectroscopy, Physical Review B. 66 (2002).
https://doi.org/10.1103/PhysRevB.66.165205

[25] S. Ramanachalam, W. B. Carter, J. P. Schaffer, T. K. Gupta, Photoluminescence study of ZnO varistor stability, Journal of Electronic Materials 24 (1995) 413-419.

[26] A.B. Djurisic, X.Y. Chen, Y.H. Leung. Recent Progress in Hydrothermal Synthesis of Zinc Oxide Nanomaterials, Recent Patents on Nanotechnology 6 (2012) 124-134.
DOI: 10.2174/187221012800270180